Ocean Acidification Alters Properties of the Exoskeleton in Adult Tanner Crabs, *Chionoecetes bairdi*

Gary H. Dickinson[1*], Shai Bejerano[1], Trina Salvador[1], Christine Makdisi[1], Shrey Patel[1], W. Christopher Long[2], Katherine M. Swiney[2,5], Robert J. Foy[2], Brittan V. Steffel[3], Kathryn E. Smith[4], and Richard B. Aronson[3]

[1]Department of Biology, The College of New Jersey, 2000 Pennington Rd., Ewing, NJ 08628, USA

[2]NOAA, National Marine Fisheries Service, Alaska Fisheries Science Center, Resource Assessment and Conservation Engineering Division, Kodiak Laboratory, 301 Research Ct., Kodiak, AK 99615, USA

[3]Department of Ocean Engineering and Marine Sciences, Florida Institute of Technology, Melbourne, FL 32901, USA

[4]The Marine Biological Association, The Laboratory, Citadel Hill, Plymouth, PL1 2PB, UK

[5]Current address: NOAA, National Marine Fisheries Service, Southwest Fisheries Science Center, Fisheries Resources Division, 8901 La Jolla Shores Dr., La Jolla, CA 92037, USA

*Corresponding author: Gary H. Dickinson, dickinga@tcnj.edu

Running Title: Acidification alters crab exoskeleton

Keywords: biomineralization; climate change; cuticle; calcite; amorphous calcium carbonate (ACC); Crustacea

SUMMARY STATEMENT

Two-year exposure of Tanner crabs to reduced-pH seawater resulted in exoskeletal alterations, including thinning, erosion, diminished claw hardness, and, in the carapace, a shift in the phase of $CaCO_3$.

ABSTRACT

Ocean acidification can affect the ability of calcifying organisms to build and maintain mineralized tissue. In decapod crustaceans, the exoskeleton is a multilayered structure composed of chitin, protein, and mineral, predominately magnesian calcite or amorphous calcium carbonate (ACC). We investigated the effects of acidification on the exoskeleton of mature (post-terminal-molt) female southern Tanner crabs, *Chionoecetes bairdi*. Crabs were exposed to one of three pH levels—8.1, 7.8, or 7.5—for two years. Reduced pH led to a suite of body-region-specific effects on the exoskeleton. Microhardness of the claw was 38% lower in crabs at pH 7.5 compared with those at pH 8.1, but carapace microhardness was unaffected by pH. In contrast, reduced pH altered elemental content in the carapace (reduced calcium, increased magnesium), but not the claw. Diminished structural integrity and thinning of the exoskeleton was observed at reduced pH in both body regions; internal erosion of the carapace was present in most crabs at pH 7.5, and the claws of these crabs showed substantial external erosion, with tooth-like denticles nearly or completely worn away. Using infrared spectroscopy, we observed a shift in the phase of calcium carbonate present in the carapace of pH-7.5 crabs: a mix of ACC and calcite was found in the carapace of crabs at pH 8.1, whereas the bulk of calcium carbonate had transformed to calcite in pH-7.5 crabs. With limited capacity for repair, the exoskeleton of long-lived crabs that undergo a terminal molt, such as C. *bairdi*, may be especially susceptible to ocean acidification.

INTRODUCTION

Decapod crustaceans possess a multifunctional exoskeleton, which serves roles in feeding, defense, desiccation-resistance, and muscle-attachment (Meyers et al., 2013; Meyers and Chen, 2014). The exoskeleton, or cuticle, is a multilayered, composite structure (Chen et al., 2008; Fabritius et al., 2011; Meyers and Chen, 2014; Fabritius et al., 2016). From interior to exterior, the cuticle is composed of four structural layers: the membranous layer, the endocuticle, the exocuticle, and the epicuticle (Travis, 1963; Roer and Dillaman, 1984). The membranous layer sits atop the hypodermis and is not mineralized (Roer and Dillaman, 1984; Fabritius et al., 2012). The endo- and exocuticle comprise the vast majority of the cuticle. These layers are composed of alpha-chitin chains, which are wrapped in protein and grouped into fibrils (Giraud-Guille, 1984; Sachs et al., 2006; Chen et al., 2008; Fabritius et al., 2011). Multiple fibrils bundle into chitin–protein fibers, which are then assembled into planes. Within the endo- and exocuticle, planes of fibers are stacked on top of one another, with each plane offset slightly with respect to the last, resulting in a Bouligand, or twisted-plywood, structure (Bouligand, 1972; Giraud-Guille, 1984; Raabe et al., 2006). Both the endo- and exocuticle layers are embedded with calcium salts, typically nanocrystalline magnesian calcite or amorphous calcium carbonate (Roer and Dillaman, 1984; Dillaman et al., 2005; Boßelmann et al., 2007). The outermost epicuticle is composed primarily of waxes and protein, interspersed with mineral aggregates (Hegdahl et al., 1977; Roer and Dillaman, 1984; Fabritius et al., 2012). The entire cuticle is shed periodically and replaced with newly-formed cuticle during the process of ecdysis, which enables growth (Travis, 1963; Roer and Dillaman, 1984). In a portion of decapod species, juveniles undergo a terminal molt to maturity, after which time full replacement of the cuticle no longer occurs (Vogt, 2012).

Structure, elemental composition, and mechanical properties of the decapod cuticle can vary among body regions (Boßelmann et al., 2007; Chen et al., 2008; Lian and Wang, 2011; Coffey et al., 2017; Steffel et al., 2019), among species (Boßelmann et al., 2007; Steffel et al., 2019; Rosen et al., 2020), and with environmental conditions (Taylor et al., 2015; Coffey et al., 2017; Glandon et al., 2018; Bednaršek et al., 2020). For example, in blue and red king crabs (*Paralithodes platypus* and *P. camtschaticus*, respectively), hardness of the claw is about twice that of the carapace, and calcium content is elevated in the claw in both species (Coffey et al., 2017). Long-term exposure to seawater with reduced pH (7.8 or 7.5) led to a 40% reduction in

hardness of the claw endocuticle in blue king crabs and a 45% reduction in claw endocuticle hardness in red king crabs (Coffey et al., 2017). Hardness of the carapace was not affected by reduced pH, but exocuticle thickness was reduced in blue king crabs.

Sensitivity to the environment is particularly relevant within the context of ocean acidification (OA), the global-scale reduction in seawater pH that has resulted from elevated atmospheric pCO_2. Since the Industrial Revolution, atmospheric pCO_2 has risen from ~280 ppm to over 410 ppm (IPCC, 2001; Raven, 2005; Dlugokencky and Trans, 2020). Dissolution of CO_2 in the world's oceans has reduced the pH of global surface waters by ~0.1 pH units since the Industrial Revolution, and based on projected CO_2 emissions scenarios, pH will drop an additional 0.3–0.5 pH units by the year 2200 (Caldeira and Wickett, 2003; Orr et al., 2005; Doney et al., 2009). At high latitudes, changes in seawater chemistry associated with OA are likely to be more extreme than at lower latitudes due to the higher solubility of CO_2 in colder waters and ocean mixing patterns (Fabry et al., 2009).

OA affects the ability of many calcifying marine organisms to build and maintain mineralized tissue (Doney et al., 2009; Kroeker et al., 2010; Kroeker et al., 2013; Sokolova et al., 2016). Reduced shell growth, shell dissolution, alterations in structure, and compromised biomechanical properties have been observed in a wide range of taxa (Orr et al., 2005; Ries et al., 2009; Byrne and Fitzer, 2019; Fitzer et al., 2019; Gaylord et al., 2019). Such changes may result from reduced pH and associated changes in acid-base homeostasis, and from the reduction in calcium carbonate saturation states (Ω) associated with OA (Ries et al., 2009; Roleda et al., 2012; Cyronak et al., 2016; Sokolova et al., 2016; Waldbusser et al., 2016). Within this body of literature, crustaceans are often reported to be less susceptible to OA than other mineralizing taxa (Ries et al., 2009; Kroeker et al., 2010; Kroeker et al., 2013; Sokolova et al. 2016; Byrne and Fitzer, 2019). Relatively high metabolic rates and iono-/ osmoregulatory capacity, protection of the site of mineralization by a waxy epicuticle, and the ability of crustaceans to employ bicarbonate within the mineralization process have all been cited as contributing to their success in tolerating OA (Wickens, 1984; Melzner et al., 2009; Ries et al., 2009; Whiteley, 2011; Sokolova et al. 2016). Systematic assessments of the effects of OA on the decapod cuticle,

however, are relatively rare; most studies limit their assessments to gross calcification rates or calcium content (e.g. Ries et al., 2009; Page et al., 2017).

The southern Tanner crab, *Chionoecetes bairdi*, is an ecologically and commercially important brachyuran decapod that inhabits the North Pacific shelf, from Oregon to the Bering Sea in Alaska. After ~3 months as larvae, juveniles settle into benthic habitats and take ~5–6 years to reach maturity (Donaldson et al., 1981). Females have a terminal molt to maturity after which they mate and extrude their first clutch of eggs. They then exhibit an annual reproductive cycle, hatching larvae in the late spring and extruding a new clutch shortly thereafter (Paul and Adams, 1984; Donaldson and Adams, 1989; Swiney, 2008). As there are no direct methods for determining the age of a decapod crustacean, it is not known how long females live after their terminal molt; however, in one study, 33% of the mature females in Cook Inlet had barnacles on them that were 3-4 years old, suggesting that many females live at least 5 years after the terminal molt (Paul and Paul, 1986). Because Tanner crab live from the subtidal down to 440 m (Jadamec, 1999), the carbonate chemistry that crabs are exposed to *in situ* almost certainly varies considerably among individuals and stocks. In the Bering Sea, the pH at 70 m depth fluctuates seasonally from a high of about 8.2 from the fall through spring to summer lows around 7.5 (Mathis et al., 2014). Crabs that live in shallower, seasonally less stratified waters, however, likely experience less dramatic pH swings. Previous OA studies with juvenile *C. bairdi* found a reduction in carapace width by 28% and an 11% reduction in calcium content of the carapace in individuals held at reduced pH (7.5) compared with crabs held under ambient pH (~8.0) (Long et al., 2013b). In adult Tanner crabs (the life-stage assessed in the current study), exposure to pH 7.5 for two years resulted in a ~29% reduction in carapace calcium, compared with crabs at ambient pH (~8.1), and the carapaces of pH-7.5 crabs were “noticeably more pliable” than crabs held at higher pH (Swiney et al., 2016).

The goal of this study was to assess the effect of OA on properties of the cuticle in mature southern Tanner crabs, *Chionoecetes bairdi*. Crabs were held at one of three pH levels, ~8.1 (ambient), 7.8, or 7.5, for two years. Given that these crabs were past their terminal molt when the exposure began, potential differences in cuticle properties reflected the crabs’ ability to maintain or repair mineralized tissue. Specifically, we quantified cuticle micromechanical

properties, thickness, structural integrity, elemental content, and the phase or polymorph of calcium carbonate (i.e. whether calcite or amorphous calcium carbonate was present). Assessments for each individual crab were conducted separately in the carapace, which protects the internal organs, and right claw, which is employed in feeding and defense. This approach allowed us to determine if the response to OA varies among body regions. Although mechanical properties of the decapod cuticle are sensitive to hydration (Hepburn et al., 1975; Joffe et al., 1975; Chen et al., 2008; Fabritius et al., 2011), the majority of studies on the decapod cuticle that have assessed mechanical properties at the micron-scale have tested samples when dry (e.g. Chen et al., 2008; Sachs et al., 2006; Coffey et al. 2017). Hence, a secondary objective was to determine if the hydration-state of the cuticle affects micro-mechanical responses to OA. Differences in the mechanics, structure, elemental content, or mineralogy of the cuticle after long-term exposure to reduced pH could affect cuticle functionality in these long-lived crabs because the post-terminal-molt-cuticle is never fully replaced.

MATERIALS AND METHODS

Animal collection and experimental exposure

Collection of crabs, experimental exposures, and seawater acidification are described in detail in Long et al. (2016) and Swiney et al. (2016). A total of 48 multiparous female adult southern Tanner crabs (*Chionoecetes bairdi*), of carapace width 98.7 mm ± 4.8 (mean ± s.d.), were caught in Chiniak Bay, Kodiak, Alaska (57° 43.25'N, 152° 17.5'W; depth ~80 m) over a 5-week period in May and June of 2011. Crab were held in ambient incoming seawater until the beginning of the experiment. Throughout the holding period crabs were fed *ad libitum* on a diet of fish and squid. Crabs were randomly assigned to one of three pH levels, ~8.1 (unmodified surface-ambient), 7.8, and 7.5, for two years, June 2011 to July 2013. The duration of the exposure was dictated by the need to capture two full reproductive cycles to examine both direct and carryover effects on the embryos and larvae (Long et al., 2016; Swiney et al., 2016); it represents an exposure time that is a substantial portion of the mature crab's life expectancy.

Exposures were conducted at the Alaska Fisheries Science Center's Kodiak Laboratory. Crabs were placed individually in 68-L tubs with 1 L min^{-1} flow of water. Water temperature was allowed to vary to mimic seasonal conditions, except that it was chilled to 9°C during the

warmest months of the summer to keep it within the range experienced by crabs *in situ*. Salinity was 31.22 PSU ± 0.47 (mean ± s.d.). Seawater was acidified using the method described by Long et al. (2013a). The method involved mixing ambient water (pumped into the laboratory from the Trident Basin at 15–26 m depth) with water from a super-acidified tank (pH 5.5, acidified via bubbling of CO_2) within a head-tank for each treatment. Mixing within the pH 7.8 and 7.5 head-tanks was controlled using Honeywell controllers and Durafet III pH probes. The ambient-treatment head-tank contained only ambient water with no input from the super-acidified tank. Measurement of pH_F and temperature were taken daily in each tub using a Durafet III pH probe (precision ± 0.03) calibrated daily with TRIS buffer (Millero, 1986). Best practices in carbonate chemistry measurements (Dickson et al., 2007) were followed throughout. Total alkalinity and dissolved inorganic carbon (DIC) were measured on water samples weekly as described in Swiney et al. (2016) per the methods in Dickson et al. (2007) and DOE (1994). Other carbonate chemistry variables were calculated in R (V2.14.0, Vienna, Austria) using the seacarb package and the default constants (Lavigne and Gattuso, 2012). Target pH levels were achieved throughout the exposure (Table 1). Saturation state with respect to calcite ($\Omega_{Calcite}$) decreased with decreasing pH and was < 1 at pH 7.5.

Throughout the experimental exposure, each crab was examined daily and fed fish and squid in excess twice a week. Each of the three pH treatments included sixteen randomly assigned crabs. Ultimately, ten survived in the ambient treatment, six in the pH-7.8 treatment, and seven in the pH-7.5 treatment (for an analysis of the survival data see Swiney et al., 2016). At the end of the two-year exposure, the surviving crabs were sacrificed. The right claw and a ~2.5-cm-square portion of the carapace, cut from the posterior margin, were immediately frozen at -80°C and shipped on dry ice to The College of New Jersey (TCNJ) for analysis. Four crabs that had died within the last 6 weeks of exposure but did not show any visible signs of exoskeletal decay were also included in analyses; all were in the pH-7.8 treatment. All cuticle samples remained frozen during transit and, upon arrival, were kept at -70°C until analysis.

Sample preparation

To prepare samples for analysis, frozen samples were first cut to size using a water-cooled diamond band-saw (Gryphon C-40). Samples were iced and kept as cold as possible during

cutting. Carapace samples were cut into four strips, each about 5 x 25 mm, for use in the assessments described below. For claw samples, the dactylus (movable finger) and pollex (fixed finger) were first cut from the manus of each claw. The entire dactyl was embedded in epoxy resin (see below), which was used for micromechanical and cuticle-thickness assessments. The pollex was further cut along its short axis to produce two segments. The first segment, consisting of ~4 mm from the manus into the pollex, was used for $CaCO_3$ polymorph assessments, whereas the remainder of the pollex was used for structural and elemental analysis. For all samples, any visible tissue adhering to the cuticle after cutting was carefully removed with forceps. Cut samples were lyophilized on a Yamato DC41-A lyophilizer for ~18 hours and then stored in a desiccator until use.

Micromechanical properties

Samples of cuticle were embedded in epoxy resin, ground, and polished for micromechanical assessments. Polishing of samples is necessary to achieve the completely level and scratch-free surface necessary for microhardness testing; for irregularly shaped cuticle samples, this is only possible when the samples are embedded in epoxy. Embedding and polishing followed the method described by Coffey et al. (2017). Individual samples were affixed to the bottom of a 3.2-cm cylindrical mounting cup. Carapace samples were oriented in such a way that grinding and polishing would reveal a cross-section along the anterior-posterior axis, and they were positioned in the mounting cup using a plastic coil-clip. Dactyl samples were positioned with the long axis parallel to the bottom of the mounting cup using a small amount of cyanoacrylate glue (Loctite® Control Gel), producing a cross-section along the longitudinal axis upon grinding and polishing. Embedding cups were filled with a two-part epoxy (Allied High Tech, EpoxySet) and left to cure at room temperature for at least 18 hours. Grinding and polishing were conducted on a manual grinding/polishing machine (Allied High Tech, M-Prep 5). Each sample was ground using a series of silicon carbide papers (180, 320, 600, and 800 grit) and then polished with a 1-μm diamond suspension and a 0.04-μm colloidal silica suspension. Samples were checked after polishing under a Jenco MET-233 metallurgical microscope and were repolished if necessary until completely flat and free of scratches. Polished samples were stored in a desiccator until testing.

Vickers microhardness was measured on a Mitutoyo HM-200 microhardness tester. Each sample was first tested dry and then was hydrated and tested again when wet. For each sample and each hydration condition, a total of 12 indents were made within the endocuticle. During the initial round of testing (dry condition), indents were spread roughly evenly along the length of the cross-section, with a spacing of at least 500 μm between indents. When samples were retested (hydrated condition), indents were placed in between those made during the first round of testing, resulting in final spacing of at least 250 μm between indents. To avoid potential edge-effects, indents were placed at least 200 μm away from layer boundaries and other structural features. This spacing was only possible within the endocuticle layer. For dactyl samples, grinding/polishing of the roughly cone-shaped dactyl resulted in a V-shaped cross-section, with the upper and lower portion of the cuticle converging at the tip. Indents were made in both the upper and lower portion of the cuticle, but, since the dactyl tips were visibly damaged in some crabs, indents in the tip region were avoided. All indents were made at 20-g load, 5-sec dwell time. Individual indents were measured directly on the hardness tester in two dimensions, and Vickers microhardness values were automatically calculated. Replicate indentations within the same sample and hydration condition were averaged to determine the mean microhardness for each sample.

Once all samples were tested in the dry condition, samples were hydrated by soaking in artificial seawater. Embedded samples were placed in a single layer in a plastic food storage container. The container was filled with artificial seawater (Instant Ocean, 35 PSU) and the samples were soaked for ~72 hours before testing in the wet condition. Samples were removed from seawater one at a time and briefly rinsed with deionized water to remove salts; visible droplets of water were removed from the sample surface using compressed air, and a series of 12 additional indents were made as described above. Indentations were made as quickly as possible once the sample was removed from water (typically within 10 minutes) to prevent dehydration. Soaking of samples was conducted in small batches (4-6 samples per batch) to ensure that the amount of time in seawater was consistent among samples. Note that it was not possible to test microhardness in cuticle samples that had never been dried, due to the need to embed samples in moisture-sensitive epoxy (see above). In mineralized tissue samples, where direct comparisons have been made between samples that were rehydrated (as described here) and those that were

never dried, no differences in micromechanical properties were observed between conditions (Baldassari et al., 2008).

Cuticle Thickness and Structural Assessment

Total cuticle thickness, which includes thickness of the endocuticle, exocuticle, and epicuticle (if visible), was quantified on the same embedded samples used for the micromechanical assessments. Each sample was imaged under a reflected light microscope (Zeiss AxioScope A1 with a Zeiss AxioCam 105 color camera). Thickness measurements were made on digital images using the camera's analysis software (Zeiss Zen 2), and at least 15 independent thickness measurements were made on each image. To determine measurement locations, a 350-μm^2 grid was placed on the digital image, and measurements were made each time the vertical grid lines crossed the sample. As in microhardness testing, replicate thickness measurements were made in both the upper and lower portions of the dactyl cross-section but were not made in the tip region. Replicate thickness measurements within the same sample were averaged to determine the mean total cuticle thickness for each sample.

Structural integrity of the cuticle was assessed semi-quantitatively using a stereomicroscope (Leica S8Apo with a Leica EC1 color camera). An unembedded segment of the carapace (cut as described in "Sample preparation") and the pollex region of the claw were used for structural assessments. Images of the interior and exterior surfaces of the carapace and of the exterior surface of the pollex were taken of each sample at a range of magnifications. Images were compared side-by-side among treatments, and deviations among samples were documented. Specifically, on the interior of the carapace, the presence or absence of erosion was assessed. The carapace interior was typically smooth and pearly white, but in a portion of samples the interior was uneven with translucent patches, which appeared dark grey under the stereomicroscope and suggested erosion of the mineralized cuticle (see Fig. 3). On the carapace exterior, discolorations and broken, uneven, or rough regions were documented. Signs of wear, resulting from prolonged abrasion, were documented and scored for pollex samples. Broken, damaged, and pitted surfaces, including on the tooth-like denticles of the pollex, were noted. Four independent evaluators assessed images of the pollex from each crab and scored each as displaying minimal, moderate,

or extensive damage as defined in Fig. S1. Images were scored without evaluators having knowledge of the exposure pH. Scores for each crab were averaged among the four evaluators.

Elemental Content

Calcium, magnesium, and strontium content were quantified using inductively coupled plasma optical emission spectrometry (ICP-OES) at the U.S. Geological Survey's Coastal and Marine Science Center, St. Petersburg, FL. Assessments were conducted using a portion of the carapace and the distal portion of the pollex, cut and lyophilized as described previously (see "Sample preparation"). Methods followed Gravinese et al. (2016) and Steffel et al. (2019). Briefly, whole samples were subjected to two rounds of oxidation, which consisted of sonication in a 1:1 mixture of 30% H_2O_2 and 0.1 M NaOH, followed by sonication in Milli-Q water. After oxidation, samples were dried overnight at 90°C and then ground to a fine powder using a mortar and pestle. Powdered samples were then subjected to an additional round of oxidation treatment (as described above), followed by drying at 90°C for at least 3 hours. Ca^{2+}, Mg^{2+}, and Sr^{2+} content was measured on powdered and oxidized samples using a PerkinElmer 7300 dual-view ICP–OES. Individual samples were weighed and acidified in 2% HNO_3 to obtain a target concentration of 20 ppm Ca^{2+}, which is compatible with the linear calibration of the instrument. Weight-percentages for each element were calculated by multiplying concentration by the volume of HNO_3 added prior to ICP-OES analysis, and then dividing by the dry weight of the sample using the conversion 1 ppm = 1 mg/L (Long et al., 2013b).

FTIR Spectroscopy: $CaCO_3$ Polymorphs

Fourier transform infrared (FTIR) spectroscopy was used to assess the phase or polymorph of calcium carbonate present in cuticle samples. A portion of the carapace and the proximal portion of the pollex, cut and lyophilized as described previously, were used for FTIR. Each sample was ground to a fine powder using a mortar and pestle. Spectra were collected using a PerkinElmer Spectrum Two spectrometer. Powdered samples were placed directly on the instrument's ATR (attenuated total reflectance) crystal and compressed with a uniform force by a built-in anvil. Spectra were taken at 4-wavenumber resolution, with 32 scans per sample. Spectra were normalized and baseline-corrected within the 700–900 cm^{-1} region, which includes the ν_2 and ν_4

peaks characteristic of $CaCO_3$ (Beniash et al., 1997; Khouzani et al., 2015). ν_2-peak position was determined using the spectrometer's analysis software (PerkinElmer Spectrum 10).

Statistical analysis

Statistical analyses were conducted using SPSS (V. 24, IBM Analytics) or R 3.1.2 (Vienna, Austria). Prior to analyses, outliers were calculated for all metrics as values greater than three times the interquartile range below or above the first or third quartile, respectively, and were removed from the dataset. Outliers were rare throughout the dataset, with no outliers identified for most assessments and a maximum of two per pH treatment for ν_2-peak position. Within the pH-7.8 treatment only, data for calcium content (carapace and claw) and ν_2-peak position (carapace) from four crabs who had died just before the conclusion of the exposure period (see "Animal collection and experimental exposure") were excluded from the dataset. For these specific metrics, a slight difference between crabs that were sacrificed at the conclusion of the experiment and those that had died just before the conclusion of the exposure period was observed (decreased carapace and calcium content, increased carapace ν_2-peak position in the crabs that died early; Mann Whitney U: $p < 0.05$). For all other metrics, there was no difference between sacrificed crabs and those that had died just before the conclusion of the exposure period. Microhardness data were analyzed using a mixed-model analysis of variance (ANOVA) at the 5% significance level. This allowed assessment of the interaction of pH (between-subject variable) and hydration (within-subject variable) on microhardness, as well as the main effects of pH and hydration individually. Mixed-model ANOVA assumptions of sphericity and equal variance were assessed using the Mauchly and Levene's tests, respectively. Other quantitative metrics—total cuticle thickness, Ca^{2+}, Mg^{2+}, and Sr^{2+} content, pollex damage, and ν_2-peak position—were assessed using one-way ANOVA followed by Tukey HSD post-hoc testing. The carapace and claw data were assessed separately. Datasets were analyzed for normality and homogeneous variances with Kolmogorov-Smirnov and Levene's tests, respectively, and data were log-transformed if necessary to meet these assumptions. If assumptions of normality or equal variance could not be met after log transforming the data, a non-parametric Kruskal–Wallis test was used in place of the parametric ANOVA. For structural integrity of the carapace, the probability of carapace erosion was fit to two models in R 3.1.2, using maximum likelihood and assuming a binomial distribution of errors, one in which the probability of erosion did not differ

among the treatments and one in which it differed among all treatments. Akaike's Information Criterion corrected for sample size, AIC_c, was calculated for each model, and the most parsimonious model was selected. Models whose AIC_cs differed by < 2 were considered to explain the data equally well (Burnham and Anderson, 2002).

RESULTS

Micromechanical Properties

Vickers microhardness was measured within the endocuticle when samples were dry and again when rehydrated. In the carapace, hydration led to a significant reduction in endocuticle hardness (Fig. 1, Tables 2, S1), with an average reduction in hardness of 60%. Hardness of the carapace was not affected by treatment pH, and the interaction of hydration and pH was not significant. In the claw, the opposite response was observed: hydration did not affect endocuticle hardness, but pH did (Fig. 1, Tables 2, S1). Hardness of the claw for crabs held at pH 7.5 was, on average, 38% lower than for those held at pH 8.1 (ambient) and 27% lower than those held at pH 7.8. The interaction of hydration and pH was not significant in the claw. Both when dry and wet, hardness of the claw was substantially higher than that of the carapace, with claw samples about four times harder than the carapace when dry and nearly 10 times higher when wet.

Cuticle Thickness and Structural Assessment

Total cuticle thickness was affected by exposure-pH in both the carapace and claw (Fig. 2, Table S2). The carapace of crabs exposed to pH 7.5 was on average 15% thinner than that of crabs at pH 8.1 (ambient). Erosion was visible on the interior of the carapace of most crabs (57%) held at pH 7.5 but never in crabs held at ambient pH (Fig. 3, Table S2). The model where the probability of carapace erosion differed among all pH treatments was a better fit and more parsimonious than the model where erosion did not differ among treatments and was therefore selected (ΔAIC_c = 4.1). Crabs at pH 7.8 had intermediate measures of total cuticle thickness and internal erosion; total cuticle thickness did not differ significantly from the pH-8.1 (ambient) or pH-7.5 crabs, and internal carapace erosion was identified in 22% of crabs. The exterior of all carapace samples assessed showed signs of wear (discolored, broken, uneven, or rough regions), and the frequency of wear did not differ among pH treatments.

For the claw, the cuticle was 31% thinner in crabs exposed to pH 7.5 compared with those at the ambient pH of 8.1 (Fig. 2, Table S2); crabs exposed to pH 7.8 were intermediate to, and did not differ from, either those at ambient pH or pH 7.5. Although patterns of wear in the form of broken, worn, or pitted surfaces were visible on the exterior of all pollex samples, the extent of pollex damage was far greater in crabs exposed to reduced pH (Fig. 3, Table S2). Particularly in pH 7.5 crabs, the contact-surface of the pollex, which displays the tooth-like denticles, was completely worn down, with the denticles barely visible (Fig. 3). In contrast, the pollex of crabs at ambient pH showed a relatively smooth appearance, with prominent denticles. Semi-quantitative assessments of pollex damage confirmed these observations, with the extent of damage greater in the pH 7.5 and 7.8 crabs compared with those at ambient pH (Table S2).

Elemental content

Calcium content of the cuticle, measured per unit dry-mass, was lower in animals held at reduced pH (7.5) in the carapace but not in the claw (Table 3). In the carapace, calcium content was reduced on average by 11% in animals exposed to pH 7.5 compared with those held at ambient pH. Calcium content for crabs at pH 7.8 did not differ from those at ambient pH. Treatment pH also exerted a significant effect on magnesium content of the carapace, but, in contrast to calcium, magnesium content increased by 17% in crabs held at pH 7.5 compared with ambient pH and by 15% compared with pH 7.8. Magnesium content did not vary significantly among pH levels in the claw. Strontium content was not affected by treatment pH in the carapace or claw (Table 3).

FTIR Spectroscopy: $CaCO_3$ Polymorphs

FTIR spectroscopy, which is sensitive to the phase of calcium carbonate present in a material, was conducted on powdered carapaces and the pollex region of the claws. Calcite is characterized by a sharp ν_2 peak at 874 cm^{-1} and a well-defined ν_4 peak at 713 cm^{-1}, whereas amorphous calcium carbonate (ACC) shows a broad ν_2 peak at 866 cm^{-1} and no ν_4 peak (Beniash et al., 1997; Khouzani et al., 2015). Figure 4 shows representative FTIR spectra for cuticle samples from crabs held at ambient (8.1) or reduced (7.5) pH, along with reference spectra for synthetic ACC (Kimmel Center for Archaeological Science Infrared Standards Library, Weizmann Institute of Science, Rehovot, Israel) and biogenic calcite (from barnacle shell:

Nardone et al., 2018). In all cases, spectra were consistent with a mix of calcite and ACC. In the carapace, there was a statistically significant shift in the position of the ν_2 peak in crabs held at pH 7.5 compared with those at ambient pH (Fig. 4, Table S2): the ν_2 peak was positioned at 866.3 ± 1.3 (mean ± s.e.m.) for animals held at ambient pH, but at 872.4 ± 0.1 for those held at pH 7.5. This shift, combined with the reduced width of the ν_2 peak at pH 7.5 and the initial formation of a ν_4 peak, suggests a transition from ACC to calcite in crabs held at pH 7.5. FTIR spectra of the claw showed a sharp ν_2 peak and a well-defined ν_4 peak, suggesting the predominance of calcite. The position of the ν_2 peak in the claw showed a very slight but statistically significant shift in the position of the ν_2 peak in crabs held at pH 7.5, compared with those at ambient pH (Fig. 4, Table S2): the ν_2 peak was positioned at 871.8 ± 0.1 for animals held at ambient pH, but at 872.2 ± 0.1 for those at pH 7.5. For both the carapace and the claw, the position of the ν_2 peak of crabs held at intermediate pH (7.8) did not differ significantly from that of crabs held at ambient pH.

DISCUSSION

The decapod cuticle is a multifunctional, composite structure that is central to the animal's success in feeding, defense, and resistance to desiccation (Meyers et al., 2013; Meyers and Chen, 2014). For animals that are past their terminal molt, functionality of the cuticle depends on maintenance of cuticle structural and mechanical integrity on scales ranging from the microscopic to the macroscopic. In decapods, the cuticle is very much a "living tissue" (Roer and Dillaman, 1984). It sits atop a multi-layered hypodermis, and cytoplasmic extensions of the outer epithelial layer of the hypodermis extend into the cuticle via pore canals (Travis, 1963; Roer and Dillaman, 1984; Cameron, 1989; Kunkel, 2013). Such intimate contact with the hypodermis may permit modification of the mineral and protein portions of the cuticle even during intermolt or after the terminal molt (Halcrow and Steel, 1992; Kunkel, 2013). Here, we aimed to assess the properties of the cuticle in the southern Tanner crab, *C. bairdi*, a long-lived inhabitant of the North Pacific shelf, in the face of reduced seawater pH—ocean acidification—and a concomitant decrease in calcite saturation state. *C. bairdi* inhabits a geographic region where the pH and calcium carbonate saturation state are already seasonally low (Long et al., 2016; Punt et al., 2016) and where future changes in ocean chemistry are likely to occur more rapidly than in

lower latitudes (Fabry et al., 2009). Two-year exposure of *C. bairdi* to reduced pH (7.5) led to a reduction in microhardness of the claw, alterations in the mineral content of the carapace, thinning of both the claw and carapace, internal dissolution of the carapace, a loss of the tooth-like denticles on claws, and a shift in the phase or polymorph of calcium carbonate present in the carapace. These changes occurred despite the fact that decapod crustaceans are often reported to be more resilient to OA than other marine calcifiers (Ries et al., 2009; Kroeker et al., 2010; Whiteley, 2011; Kroeker et al., 2013; Byrne and Fitzer, 2019).

Microhardness is a measure of a material's resistance to mechanical (plastic) deformation. Assessments of microhardness within the *C. bairdi* endocuticle revealed two general patterns. First, microhardness of the claw was consistently higher than that of the carapace, regardless of seawater pH, a pattern previously observed in a number of other decapod crab species (Lian and Wang, 2011; Steffel et al., 2019). Second, long-term exposure of crabs to reduced-pH seawater resulted in a body-region-specific reduction in microhardness. Although a significant reduction in endocuticle microhardness was observed in the claw, the effect of reduced pH on microhardness of the carapace was not significant. The body-region-specific response to seawater pH observed here is consistent with previous assessments of juvenile blue and red king crabs, *P. platypus* and *P. camtschaticus*, in which a reduction in endocuticle microhardness was also observed for the claw, but not the carapace (Coffey et al., 2017). In the Coffey et al. (2017) study, crabs had molted several times during experimental exposure. Together with our results, these findings suggest that exposure to reduced-pH seawater induces a similar pattern of changes in cuticle mechanical properties, whether the cuticle is newly deposited during ecdysis, or if it is pre-existing when exposure begins.

The harder endocuticle of the claw compared with the carapace may result from elevated calcium content (Sachs et al., 2006; Waugh et al., 2006; Boßelmann et al., 2007; Page et al., 2017): on average, claw samples contained ~40% more calcium than those from the carapace. The phase of calcium carbonate present within these cuticle regions may also contribute. The proportion of calcite versus ACC is greater in the claw than the carapace, and calcite tends to be harder than ACC (Bentov et al., 2016a). Neither calcium content nor the phase of calcium carbonate, though, can adequately explain the reduction in hardness observed in the claws of crabs exposed to

reduced pH. Calcium content of the claw did not differ significantly among pH treatments, and claws from all pH levels are composed primarily of calcite. This observation is again consistent with the work of Coffey et al. (2017) on *P. platypus* and *P. camtschaticus*. Despite a reduction in endocuticle hardness in both species at reduced pH, calcium content was not affected by exposure pH in *P. platypus*, and in *P. camtschaticus,* calcium content of the claw was actually greater at reduced pH. A number of other properties can influence cuticle hardness in decapods, including: the packing density of twisted plywood structures; phosphate content (including the presence of calcium phosphate); cross-linking and other modifications of the protein portion; density of pore canals; and the orientation, density, and structural integrity of mineralized protein-chitin fibers (Melnick et al., 1996; Chen et al., 2008; Fabritius et al., 2011; Lian and Wang, 2011; Fabritius et al., 2012; Bentov et al., 2016a; Bentov et al., 2016b; Rosen et al., 2020). It remains to be determined which, if any, of these properties are driving the observed reduction in claw microhardness at reduced seawater pH seen here and by Coffey et al. (2017).

The decapod cuticle is hydrated in its natural state (Hepburn et al., 1975; Cameron and Wood, 1985; Boßelmann et al., 2007; Neues et al., 2007). Cameron and Wood (1985) estimated that 26.5% of the *Callinectes sapidus* carapace was water, based on wet and dry masses. Using thermogravimetry (TGA), Boßelmann et al. (2007) identified 11.8% of the carapace of *Cancer pagurus* as water, whereas the dactylus of the claw contained only 1% water. The difference in hydration of the carapace versus the dactylus, along with the elevated calcium content in the claw, may explain the difference in sensitivity to hydration observed here (Vincent, 2002; Fabritius et al., 2011). The microhardness of carapace samples when tested dry was about three times higher than when the same samples were tested wet, whereas microhardness of the dactylus was not affected by hydration. Importantly, the response of the cuticle in terms of microhardness to reduced pH was not affected by hydration state (i.e. the interaction of pH and hydration within the repeated measures ANOVA was not statistically significant for the carapace or claw; see Table 2). Hence, the structural or chemical properties of the cuticle that drive body-region-specific changes in microhardness with pH do not appear to be affected by hydration.

Long-term exposure of *C. bairdi* to reduced pH resulted in a suite of potentially interrelated alterations in the cuticle of the carapace. At pH 7.5, calcium content was reduced, while

magnesium content was elevated, implying a higher ratio of Mg^{2+}:Ca^{2+}. Thickness of the carapace was reduced at pH 7.5, and the majority of pH-7.5 carapace samples showed internal erosion. Solubility of calcite tends to increase with elevated Mg^{2+}:Ca^{2+} (Morse et al., 2006; Andersson et al., 2008), which may have left the cuticle more susceptible to internal dissolution (Bednaršek et al., 2020). Observed internal dissolution could in turn have driven the reduction in thickness of the carapace cuticle. It is possible that the reduction in carapace calcium results from mobilization of Ca^{2+} and HCO_3^- from the cuticle, as a mechanism to buffer hemolymph pH (DeFur et al., 1980; Henry et al., 1981; Cameron, 1985; Spicer et al., 2007; Page et al., 2017; Bednaršek et al., 2020). Indeed, when Meseck et al. (2016) assessed extracellular hemolymph pH (pH_e) in the same *C. bairdi* assessed here, pH_e was maintained at ~8.09 even in crabs held at the lowest seawater pH. It is important to note, however, that the contribution of carapace ions to hemolymph buffering in other crab species appears to be minor compared with the uptake of ions from external seawater (Cameron, 1985; Spicer et al., 2007).

In the claw, exposure to reduced pH resulted in thinning of the cuticle without a corresponding change in elemental content. Internal dissolution could not be readily assessed in claw samples, but extensive erosion of the exterior of the pollex was observed in crabs held at pH 7.5, with nearly complete loss of the tooth-like denticles in these crabs. This occurred despite the fact that the captive crabs were fed soft foods and hence did not experience the high levels of abrasion they might have experienced in the field from consuming heavily calcified foods and interacting with other crabs. The waxy epicuticle in decapods protects the underlying mineral from changes in seawater chemistry (Ries et al., 2009). As shown by Kunkel et al. (2012), removal of the epicuticle leads to an increase in ion flux from the mineralized cuticle. Waugh et al. (2006) and Rosen et al. (2020) documented in multiple crab species that normal wear on the denticles results in loss of the epicuticle, as well as the exocuticle, from the denticle surface, which could leave the mineralized endocuticle susceptible to dissolution. The presence of epicuticle on the denticle surface was not assessed before exposure in our study, but given that the crabs used here were already past their terminal molt when collected from the field, it is likely that the epicuticle covering the denticles was absent at the start of the experimental exposure. Damage to the claw, and particularly to the tooth-like denticles, may lead to a reduction in the crabs' prey-capture efficiency (Juanes and Hartwick, 1990).

The interior dissolution of the *C. bairdi* carapace and exterior dissolution and wear of the claw show promise as ecosystem indicators (*sensu* Kershner et al., 2011) for ocean acidification effects in Alaska. Scoring of both could be done on a semi-quantitative scale and could easily be incorporated into existing annual surveys that target *C. bairdi*, an economically-important species. These measures are correlated with other significant negative outcomes such as embryonic mortality and decreased female survival (Swiney et al., 2016) that are harder to measure or estimate on an annual basis. As a next step in developing these metrics as ecosystem indicators, future work should examine variation in cuticle dissolution and wear in natural populations to determine if they are correlated with natural environmental gradients.

Multiple mineral forms and phases are found within the decapod cuticle, with the mineral component being predominately nanocrystalline calcite and ACC (Roer and Dillaman, 1984; Dillaman et al., 2005; Fabritius et al., 2012). After molting, calcium carbonate is initially deposited as ACC, and some (but not all) of the ACC is transformed to calcite in the days following initial mineral deposition. Stabilization of ACC (i.e. the inhibition of calcite nucleation) may involve protein components of the cuticle, specific ions (magnesium, phosphorus, and silicon), and glycolytic intermediates (PEP and 3PG) (Coblentz et al., 1998; Addadi et al., 2003; Weiner et al., 2003; Sato et al., 2011; Roer and Dillaman, 2018). Given that ACC is highly unstable (Weiner and Addadi, 1997; Addadi et al., 2003; Weiner et al., 2003), a slight change in conditions within the cuticle could result in calcite nucleation.

FTIR spectroscopy of the *C. bairdi* carapace suggests a shift in the phase of calcium carbonate from ACC to calcite. To the best of our knowledge, this is the first report of a shift in mineral phase in a crustacean (Ries, 2011). Benefits of the use of ACC have been discussed in depth (Addadi et al., 2003; Weiner et al., 2003; Neues et al., 2007; Bentov et al., 2016a); ACC is isotropic and fracture-resistant, and it can serve as a readily-soluble Ca^{2+} pool. The functional implications of this shift in mineral phase remain to be determined. At least at the micron-scale, the shift toward calcite did not appear to affect hardness (i.e. microhardness was not affected by exposure pH), but isotropy and fracture-resistance were not directly assessed. Continued quantification of cuticle mechanical properties at a range of spatial scales (from the nano-scale to

548 the scale of the entire carapace) and temporal scales (from short to extended times since molting
549 and durations of pH exposure), as well as assessment of the role of carapace ions in hemolymph
550 buffering, may help to resolve the functional consequences of the observed shift in mineralogy.
551
552 **5. Conclusions**
553 Variations in mechanical, elemental, structural, and mineralogical properties of the decapod-crab
554 exoskeleton lead to differences in functionality. This is clearly evident when comparing the
555 carapace with the claw, which is the primary feeding and active defensive structure. Compared
556 with the carapace, the claw is substantially harder, and it contains more calcium but less
557 magnesium. A greater proportion of calcium carbonate in the claw is present as crystalline
558 calcite as opposed to ACC, and the cuticle of the claw is less sensitive to hydration. These
559 differences set the stage for the body-region-specific response to ocean acidification observed in
560 *C. bairdi.* Exposure to reduced pH led to a reduction in microhardness of the claw, but not the
561 carapace. There was no change in elemental content at reduced pH in the claw, but in the
562 carapace calcium content was reduced and magnesium content increased. Calcium carbonate in
563 the claw was already predominantly in the form of calcite, whereas in the carapace, calcium
564 carbonate was primarily ACC at ambient pH but shifted to calcite in crabs exposed to pH 7.5.
565
566 Assessment of the structural integrity of the cuticle suggests that long-lived crabs that display
567 determinate growth may be particularly susceptible to ocean acidification. *C. bairdi* held at a
568 reduced pH of 7.5 displayed internal dissolution of the carapace, as well as extensive erosion of
569 the claw, with nearly complete loss of tooth-like denticles. At the functional level, the loss of
570 denticles could inhibit feeding ability and efficiency, as has been shown in other crabs (Juanes
571 and Hartwick, 1990). Although direct assessments of the effect of degraded claws on feeding in
572 *C. bairdi* are still needed, impaired feeding could lead to energy limitation with potential
573 consequences on reproductive output. The thinner, eroded cuticle observed in both body regions
574 may also break more readily, diminishing its protective functionality. Although cuticle repair is
575 possible after the terminal molt (Halcrow and Steel, 1992), the cuticle is never fully replaced as
576 occurs during molting. Even under current oceanic conditions, cuticle damage tends to
577 accumulate over time, leading to a decrease in shell condition with age (Ernst et al., 2005;
578 Fonseca et al., 2008; Vogt, 2012). Furthermore, in *C. bairdi,* the hemocytes responsible for

579 cuticle repair (granular and semi-granular cells) show reduced intracellular pH (pH_i), which may
580 limit their functionality in the cuticle-repair process (Meseck et al., 2016). Altogether, the results
581 presented here demonstrate that ocean acidification can alter exoskeleton properties in *C. bairdi*,
582 which may affect the success of this ecologically and economically important species in coming
583 years.
584
585 **Acknowledgments**
586 We thank Tait Algayer, Natasha Chaudhari, Teresa Dinh, and Luisandra Lugo for evaluating the
587 images, and Dr. Rebecca Metzler for discussions on FTIR spectroscopy. The scientific results
588 and conclusions, as well as any views or opinions expressed herein, are those of the author(s) and
589 do not necessarily reflect those of NOAA or the Department of Commerce. Reference to trade
590 names does not imply endorsement by the National Marine Fisheries Service, NOAA. This is
591 contribution no. 233 from the Institute for Global Ecology at the Florida Institute of Technology.
592
593 **Competing interests**
594 The authors declare no competing or financial interests.
595
596 **Author contributions**
597 Conceptualization: G.H.D., W.C.L., R.J.F.; Methodology: G.H.D., W.C.L., R.J.F., K.E.S.,
598 R.B.A.; Formal analysis: G.H.D, W.C.L.; Investigation: G.H.D., S.B., T.S., C.M., S.P., W.C.L.,
599 K.M.S., B.V.S.; Resources: G.H.D., W.C.L., R.J.F., R.B.A.; Writing, original draft: G.H.D.,
600 W.C.L.; Writing, review & editing: G.H.D., S.B., T.S., C.M., S.P., W.C.L., K.M.S., R.J.F,
601 B.V.S., K.E.S., R.B.A.; Visualization: G.H.D.; Supervision: G.H.D., W.C.L., R.J.F., R.B.A.;
602 Project administration: G.H.D., W.C.L., R.J.F., R.B.A.; Funding acquisition: G.H.D., W.C.L.,
603 R.J.F., R.B.A.
604
605 **Funding**
606 This project was partially funded by the North Pacific Research Board (Project #1010, grant to
607 R.J.F., W.C.L, & K.M.S.), the National Oceanic and Atmospheric Administration (NOAA)
608 Ocean Acidification Program (W.C.L. & R.J.F.), and the U.S. National Science Foundation

(grants DMR-1905466 to G.H.D. and ANT-1141877 to R.B.A.). S.B. and S.P. were supported by The College of New Jersey's Mentored Undergraduate Research Experience (MUSE).

Data availability

Data are available from the Dryad digital repository.

References

Addadi, L., Raz, S. and Weiner, S. (2003). Taking advantage of disorder: amorphous calcium carbonate and its roles in biomineralization. *Adv. Mater.* **15**, 959-970.

Andersson, A. J., Mackenzie, F. T. and Bates, N. R. (2008). Life on the margin: implications of ocean acidification on Mg-calcite, high latitude and cold-water marine calcifiers. *Mar. Ecol. Prog. Ser.* **373**, 265-273.

Baldassarri, M., Margolis, H.C., and Beniash, E. (2008). Compositional determinants of mechanical properties of enamel. *J. Dent. Res.* **87**, 645-649.

Bednaršek, N., Feely, R. A., Beck, M. W., Alin, S. R., Siedlecki, S. A., Calosi, P., Norton, E. L., Saenger, C., Štrus, J. and Greeley, D. (2020). Exoskeleton dissolution with mechanoreceptor damage in larval Dungeness crab related to severity of present-day ocean acidification vertical gradients. *Sci. Total Environ.* **716**, 136610.

Beniash, E., Aizenberg, D., Addadi, L. and Weiner, S. (1997). Amorphous calcium carbonate transforms into calcite during sea urchin larval spicule growth. *P. Roy. Soc. B* **264**, 461-465.

Bentov, S., Abehsera, S. and Sagi, A. (2016a). The mineralized exoskeletons of crustaceans. In *Extracellular Composite Matrices in Arthropods* (ed. E. Cohen and B. Moussian), pp. 137-163. Cham, Switzerland: Springer.

Bentov, S., Aflalo, E. D., Tynyakov, J., Glazer, L. and Sagi, A. (2016b). Calcium phosphate mineralization is widely applied in crustacean mandibles. *Sci. Rep.* **6**, 22118.

Boßelmann, F., Romano, P., Fabritius, H., Raabe, D. and Epple, M. (2007). The composition of the exoskeleton of two crustacea: The American lobster *Homarus americanus* and the edible crab *Cancer pagurus*. *Thermochim. Acta* **463**, 65-68.

Bouligand, Y. (1972). Twisted fibrous arrangements in biological materials and cholesteric mesophases. *Tissue Cell* **4**, 189-217.

Burnham, K. P. and Anderson, D. R. (2002). *Model Selection and Multi-Model Inference: a Practical Information-Theoretic Approach*. New York: Springer Science + Business Media.

Byrne, M. and Fitzer, S. (2019). The impact of environmental acidification on the microstructure and mechanical integrity of marine invertebrate skeletons. *Conserv. Physiol.* **7**, coz062.

Caldeira, K. and Wickett, M. E. (2003). Anthropogenic carbon and ocean pH. *Nature* **425**, 365-365.

Cameron, J. N. (1985). Compensation of hypercapnic acidosis in the aquatic blue crab, *Callinectes sapidus*: the predominance of external sea water over carapace carbonate as the proton sink. *J. Exp. Biol.* **114**, 197-206.

Cameron, J. N. (1989). Post-moult calcification in the blue crab, *Callinectes sapidus*: timing and mechanism. *J. Exp. Biol.* **143**, 285-304.

Cameron, J. N. and Wood, C. M. (1985). Apparent H^+ excretion and CO_2 dynamics accompanying carapace mineralization in the blue brab (*Callinectes sapidus*) following molting. *J. Exp. Biol.* **114**, 181-196.

Chen, P.-Y., Lin, A. Y.-M., McKittrick, J. and Meyers, M. A. (2008). Structure and mechanical properties of crab exoskeletons. *Acta Biomater.* **4**, 587-596.

Coblentz, F. E., Shafer, T. H. and Roer, R. D. (1998). Cuticular proteins from the blue crab alter in vitro calcium carbonate mineralization. *Comp. Biochem. Physiol. B Biochem Mol. Biol.* **121**, 349-360.

Coffey, W. D., Nardone, J. A., Yarram, A., Long, W. C., Swiney, K. M., Foy, R. J. and Dickinson, G. H. (2017). Ocean acidification leads to altered micromechanical properties of the mineralized cuticle in juvenile red and blue king crabs. *J. Exp. Mar. Biol. Ecol.* **495**, 1-12.

Cyronak, T., Schulz, K. G. and Jokiel, P. L. (2016). The Omega myth: what really drives lower calcification rates in an acidifying ocean. *ICES J. Mar. Sci.* **73**, 558-562.

DeFur, P., Wilkes, P. and McMahon, B. (1980). Non-equilibrium acid-base status in *C. productus*: role of exoskeletal carbonate buffers. *Resp. Physiol.* **42**, 247-261.

Dickson, A. G., Sabine, C. L., and Christian, J. R. (2007). Guide to best practices for ocean CO_2 measurements. PICES Special Publication **3**: 191 p.

Dillaman, R., Hequembourg, S. and Gay, M. (2005). Early pattern of calcification in the dorsal carapace of the blue crab, *Callinectes sapidus*. *J. Morphol.* **263**, 356-374.

Dlugokencky, E. and Trans, P. (2020). Data from NOAA global monitoring laboratory. http://www.esrl.noaa.gov/gmd/ccgg/trends/global.html.

DOE. (1994). Handbook of methods for the analysis of the various parameters of the carbon dioxide system in sea water. Version 2. ORNL/CDIAC-74: 197 p.

Donaldson, W. E., and Adams, A. E. (1989). Ethogram of behavior with emphasis on mating for the Tanner crab *Chionoecetes bairdi* Rathbun. *J. Crust. Biol.* **9**, 37-53.

Doney, S. C., Fabry, V. J., Feely, R. A. and Kleypas, J. A. (2009). Ocean acidification: the other CO_2 problem. *Annu. Rev. Mar. Sci.* **1**, 169-192.

Ernst, B., Orensanz, J. M. and Armstrong, D. A. (2005). Spatial dynamics of female snow crab (*Chionoecetes opilio*) in the eastern Bering Sea. *Can. J. Fish. Aquat. Sci.* **62**, 250-268.

Fabritius, H., Sachs, C., Raabe, D., Nikolov, S., Friák, M. and Neugebauer, J. (2011). Chitin in the exoskeletons of arthropoda: From ancient design to novel materials science. In *Chitin: Formation and Diagenesis* (ed. N. S. Gupta), pp. 35-60. Berlin, Germany: Springer.

Fabritius, H.-O., Karsten, E. S., Balasundaram, K., Hild, S., Huemer, K. and Raabe, D. (2012). Correlation of structure, composition and local mechanical properties in the dorsal carapace of the edible crab *Cancer pagurus*. *Z. Krist.-Cryst. Mater.* **227**, 766-776.

Fabritius, H.-O., Ziegler, A., Friák, M., Nikolov, S., Huber, J., Seidl, B. H., Ruangchai, S., Alagboso, F. I., Karsten, S. and Lu, J. (2016). Functional adaptation of crustacean exoskeletal elements through structural and compositional diversity: a combined experimental and theoretical study. *Bioinspir. Biomim.* **11**, 055006.

Fabry, V. J., McClintock, J. B., Mathis, J. T. and Grebmeier, J. M. (2009). Ocean acidification at high latitudes: the bellwether. *Oceanogr.* **22**, 160-171.

Fitzer, S. C., Chan, V., Meng, Y., Rajan, L., Suzuki, M., Not, C., Toyofuko, T., Falkenberg, L., Byrne, M. and Harvey, B. P. (2019). Established and emerging techniques for characterising the formation, structure and performance of calcified structures under ocean acidification. *Oceanogr. Mar. Biol.* **57**, 89-126.

Fonseca, D. B., Sainte-Marie, B. and Hazel, F. (2008). Longevity and change in shell condition of adult male snow crab *Chionoecetes opilio* inferred from dactyl wear and mark-recapture data. *Trans. Am. Fish. Soc.* **137**, 1029-1043.

Gaylord, B., Barclay, K. M., Jellison, B. M., Jurgens, L. J., Ninokawa, A. T., Rivest, E. B. and Leighton, L. R. (2019). Ocean change within shoreline communities: from biomechanics to behaviour and beyond. *Conserv. Physiol.* **7**, coz077.

Giraud-Guille, M.-M. (1984). Fine structure of the chitin-protein system in the crab cuticle. *Tissue Cell* **16**, 75-92.

Glandon, H. L., Kilbourne, K. H., Schijf, J. and Miller, T. J. (2018). Counteractive effects of increased temperature and pCO_2 on the thickness and chemistry of the carapace of juvenile blue crab, *Callinectes sapidus*, from the Patuxent River, Chesapeake Bay. *J. Exp. Mar. Biol. Ecol.* **498**, 39-45.

Gravinese, P. M., Flannery, J. A. and Toth, L. T. (2016). A methodology for quantifying trace elements in the exoskeletons of Florida stone crab (*Menippe Mercenaria*) larvae using inductively coupled plasma optical emission spectrometry (ICP-OES): U.S. Geological Survey Open-File Report 2016–1148, 12 p., https://doi.org/10.3133/ofr20161148.

Halcrow, K. and Steel, C. (1992). Cuticular repair in the mature male snow crab, *Chionoecetes opilio* (Majidae; Crustacea): relation to ecdysteroids. *Can. J. Zool.* **70**, 314-319.

Hegdahl, T., Gustavsen, F. and Silness, J. (1977). The structure and mineralization of the carapace of the crab (*Cancer pagurus* L.) 3. The epicuticle. *Zool. Scr.* **6**, 215-220.

Henry, R., Kormanik, G., Smatresk, N. and Cameron, J. (1981). The role of $CaCO_3$ dissolution as a source of HCO_3^- for the buffering of hypercapnic acidosis in aquatic and terrestrial decapod crustaceans. *J. Exp. Biol.* **94**, 269-274.

Hepburn, H., Joffe, I., Green, N. and Nelson, K. (1975). Mechanical properties of a crab shell. *Comp. Biochem. Physiol. A Physiol.* **50**, 551-554.

IPCC. (2001). *Climate Change 2001–IPCC Third Assessment Report*. Cambridge, UK: Cambridge University Press.

Jadamec, L., Donaldson, W., and Cullenberg, P. (1999). *Biological Field Techniques for* Chionoecetes *Crabs*. Fairbanks, USA: Alaska Sea Grant College Program, University of Alaska.

Joffe, I., HR, H. and KJ, N. (1975). Mechanical properties of a crustacean exoskeleton. *Comp. Biochem. Physiol. A Physiol.* **50**, 545-549.

Juanes, F. and Hartwick, E. (1990). Prey size selection in Dungeness crabs: the effect of claw damage. *Ecology* **71**, 744-758.

Kershner, J., Samhouri, J. F., James, C. A. and Levin, P. S. (2011). Selecting indicator portfolios for marine species and food webs: a Puget Sound case study. *PLoS One* **6**, e25248.

Khouzani, M. F., Chevrier, D. M., Güttlein, P., Hauser, K., Zhang, P., Hedin, N. and Gebauer, D. (2015). Disordered amorphous calcium carbonate from direct precipitation. *CrystEngComm* **17**, 4842-4849.

Kroeker, K. J., Kordas, R. L., Crim, R. N. and Singh, G. G. (2010). Meta-analysis reveals negative yet variable effects of ocean acidification on marine organisms. *Ecol. Lett.* **13**, 1419-1434.

Kroeker, K. J., Kordas, R. L., Crim, R., Hendriks, I. E., Ramajo, L., Singh, G. S., Duarte, C. M. and Gattuso, J. P. (2013). Impacts of ocean acidification on marine organisms: quantifying sensitivities and interaction with warming. *Glob. Chang. Biol.* **19**, 1884-1896.

Kunkel, J. G. (2013). Modeling the calcium and phosphate mineralization of American lobster cuticle. *Can. J. Fish. Aquat. Sci.* **70**, 1601-1611.

Kunkel, J. G., Nagel, W. and Jercinovic, M. J. (2012). Mineral fine structure of the American lobster cuticle. *J. Shellfish. Res.* **31**, 515-526.

Lavigne, H., and Gattuse, J. (2012). seacarb: Seawater carbonate chemistry with R. http://CRAN.R-project.org/package=seacarb. R package version 2.4.6 edn.

Lian, J. and Wang, J. (2011). Microstructure and mechanical properties of dungeness crab exoskeletons. In *Mechanics of Biological Systems and Materials, Volume 2*, (ed. T. Proulx), pp. 93-99. New York: Springer.

Long, W. C., Swiney, K. M. and Foy, R. J. (2013a). Effects of ocean acidification on the embryos and larvae of red king crab, *Paralithodes camtschaticus*. *Mar. Pollut. Bull.* **69**, 38-47.

Long, W. C., Swiney, K. M. and Foy, R. J. (2016). Effects of high pCO_2 on Tanner crab reproduction and early life history, Part II: carryover effects on larvae from oogenesis and embryogenesis are stronger than direct effects. *ICES J. Mar. Sci.* **73**, 836-848.

Long, W. C., Swiney, K. M., Harris, C., Page, H. N. and Foy, R. J. (2013b). Effects of ocean acidification on juvenile red king crab (*Paralithodes camtschaticus*) and Tanner crab (*Chionoecetes bairdi*) growth, condition, calcification, and survival. *PLoS One* **8**, e60959.

Mathis, J. T., Cross, J. N., Monacci, N., Feely, R. A., and Stabeno, P. (2014). Evidence of prolonged aragonite undersaturations in the bottom waters of the southern Bering Sea shelf from autonomous sensors. *Deep Sea Res. Part II Top. Stud. Oceanogr*. **109**, 125-133.

Melzner, F., Gutowska, M.A., Langenbuch, M., Dupont, S., Lucassen, M., Thorndyke, M.C., Bleich, M., and Portner, H.O. (2009). Physiological basis for high CO_2 tolerance in marine ectothermic animals: pre-adaptation through lifestyle and ontogeny? *Biogeosciences* **6**, 2313-2331.

764 **Melnick, C., Chen, Z. and Mecholsky, J.** (1996). Hardness and toughness of exoskeleton
765 material in the stone crab, *Menippe mercenaria*. *J. Mater. Res.* **11**, 2903-2907.

766 **Meseck, S. L., Alix, J. H., Swiney, K. M., Long, W. C., Wikfors, G. H. and Foy, R. J.** (2016).
767 Ocean acidification affects hemocyte physiology in the Tanner crab (*Chionoecetes bairdi*). *PLoS*
768 *One* **11**, e0148477.

769 **Meyers, M. A. and Chen, P.-Y.** (2014). *Biological Materials Science: Biological Materials,*
770 *Bioinspired Materials, and Biomaterials* Cambridge, UK: Cambridge University Press.

771 **Meyers, M. A., McKittrick, J. and Chen, P.-Y.** (2013). Structural biological materials: critical
772 mechanics-materials connections. *Science* **339**, 773-779.

773 **Millero, F. J.** (1986). The pH of estuarine waters. *Limnol. Oceanogr.* **31**, 839-847.

774 **Morse, J. W., Andersson, A. J. and Mackenzie, F. T.** (2006). Initial responses of carbonate-
775 rich shelf sediments to rising atmospheric pCO_2 and "ocean acidification": role of high Mg-
776 calcites. *Geochim. Cosmochim. Acta* **70**, 5814-5830.

777 **Nardone, J. A., Patel, S., Siegel, K. R., Tedesco, D., McNicholl, C. G., O'Malley, J., Herrick,**
778 **J., Metzler, R. A., Orihuela, B., Rittschof, D, and Dickinson, G. H.** (2018). Assessing the
779 impacts of ocean acidification on adhesion and shell formation in the barnacle *Amphibalanus*
780 *amphitrite*. *Front. Mar. Sci.* **5**, 369.

781 **Neues, F., Ziegler, A. and Epple, M.** (2007). The composition of the mineralized cuticle in
782 marine and terrestrial isopods: a comparative study. *CrystEngComm* **9**, 1245-1251.

783 **Orr, J. C., Fabry, V. J., Aumont, O., Bopp, L., Doney, S. C., Feely, R. A., Gnanadesikan,**
784 **A., Gruber, N., Ishida, A., Joos, F. et al.** (2005). Anthropogenic ocean acidification over the
785 twenty-first century and its impact on calcifying organisms. *Nature* **437**, 681-686.

786 **Page, T. M., Worthington, S., Calosi, P. and Stillman, J. H.** (2017). Effects of elevated pCO_2
787 on crab survival and exoskeleton composition depend on shell function and species distribution:
788 a comparative analysis of carapace and claw mineralogy across four porcelain crab species from
789 different habitats. *ICES J. Mar. Sci.* **74**, 1021-1032.

790 **Paul, A. J., and Adams, A. E.** (1984). Breeding and fertile period for female *Chionoecetes*
791 *bairdi* (Decapoda, Majidae). *J. Crust. Biol*. **4**, 589-594.

792 **Paul, J., and Paul, A.** (1986). *Encrusting Barnacles as Ageable Tags on Gulf of Alaska*
793 *Chionoecetes bairdi (Decapoda)*. Fairbanks, USA: Alaska Sea Grant College Program,
794 University of Alaska.

795 **Punt, A. E., Foy, R. J., Dalton, M. G., Long, W. C. and Swiney, K. M.** (2016). Effects of
796 long-term exposure to ocean acidification conditions on future southern Tanner crab
797 (*Chionoecetes bairdi*) fisheries management. *ICES J. Mar. Sci.* **73**, 849-864.

798 **Raabe, D., Romano, P., Sachs, C., Fabritius, H., Al-Sawalmih, A., Yi, S.-B., Servos, G. and**
799 **Hartwig, H.** (2006). Microstructure and crystallographic texture of the chitin–protein network in
800 the biological composite material of the exoskeleton of the lobster *Homarus americanus*. *Mater.*
801 *Sci. Eng. A* **421**, 143-153.

802 **Raven, J.** (2005). *Ocean Acidification Due to Increasing Atmospheric Carbon Dioxide.* London,
803 UK: The Royal Society.

Ries, J. B. (2011). Skeletal mineralogy in a high-CO_2 world. *J. Exp. Mar. Biol. Ecol.* **403**, 54-64.

Ries, J. B., Cohen, A. L. and McCorkle, D. C. (2009). Marine calcifiers exhibit mixed responses to CO_2-induced ocean acidification. *Geology* **37**, 1131-1134.

Roer, R. and Dillaman, R. (1984). The structure and calcification of the crustacean cuticle. *Am. Zool.* **24**, 893-909.

Roer, R. D. and Dillaman, R. M. (2018). The initiation and early stages of postmolt mineralization in the blue crab, *Callinectes sapidus*. *Front. Mar. Sci.* **5**, 151.

Roleda, M. Y., Boyd, P. W. and Hurd, C. L. (2012). Before ocean acidification: calcifier chemistry lessons. *J. Phycol.* **48**, 840-843.

Rosen, M. N., Baran, K. A., Sison, J. N., Steffel, B. V., Long, W. C., Foy, R. J., Smith, K. E., Aronson, R. B. and Dickinson, G. H. (2020). Mechanical resistance in decapod claw denticles: contribution of structure and composition. *Acta Biomater.* **110**, *196-207*.

Sachs, C., Fabritius, H. and Raabe, D. (2006). Hardness and elastic properties of dehydrated cuticle from the lobster *Homarus americanus* obtained by nanoindentation. *J. Mater. Res.* **21**, 1987-1995.

Sato, A., Nagasaka, S., Furihata, K., Nagata, S., Arai, I., Saruwatari, K., Kogure, T., Sakuda, S. and Nagasawa, H. (2011). Glycolytic intermediates induce amorphous calcium carbonate formation in crustaceans. *Nat. Chem. Biol.* **7**, 197-199.

Sokolova, I. M., Matoo, O. B., Dickinson, G. H. and Beniash, E. (2016). Physiological effects of ocean acidification on animal calcifiers. In *Stressors in the Marine Environment: Physiological and Ecological Responses and Societal Implications*, (ed. M. Solan and N. M. Whiteley), pp. 36-55. Oxford, UK: Oxford University Press.

Spicer, J. I., Raffo, A. and Widdicombe, S. (2007). Influence of CO_2-related seawater acidification on extracellular acid-base balance in the velvet swimming crab *Necora puber*. *Mar. Biol.* **151**, 1117-1125.

Steffel, B. V., Smith, K. E., Dickinson, G. H., Flannery, J. A., Baran, K. A., Rosen, M. N., McClintock, J. B. and Aronson, R. B. (2019). Characterization of the exoskeleton of the Antarctic king crab *Paralomis birsteini*. *Invertebr. Biol*. **138**, e12246.

Swiney, K. M. (2008). Egg extrusion, embryo development, timing and duration of eclosion, and incubation period of primiparous and multiparous tanner crabs (*Chionoecetes bairdi*). *J. Crust. Biol*. **28**, 334-341.

Swiney, K. M., Long, W. C. and Foy, R. J. (2016). Effects of high pCO_2 on Tanner crab reproduction and early life history—Part I: long-term exposure reduces hatching success and female calcification, and alters embryonic development. *ICES J. Mar. Sci.* **73**, 825-835.

Taylor, J. R., Gilleard, J. M., Allen, M. C. and Deheyn, D. D. (2015). Effects of CO_2-induced pH reduction on the exoskeleton structure and biophotonic properties of the shrimp *Lysmata californica*. *Sci. Rep.* **5**, 10608.

Travis, D. F. (1963). Structural features of mineralization from tissue to macromolecular levels of organization in the decapod Crustacea. *Ann. NY Acad. Sci.* **109**, 177-245.

Vincent, J. F. (2002). Arthropod cuticle: a natural composite shell system. *Compos. A Appl. Sci. Manuf.* **33**, 1311-1315.

Vogt, G. (2012). Ageing and longevity in the Decapoda (Crustacea): a review. *Zool. Anzeiger.* **251**, 1-25.

Waldbusser, G. G., Hales, B. and Haley, B. A. (2016). Calcium carbonate saturation state: on myths and this or that stories. *ICES J. Mar. Sci.* **73**, 563-568.

Waugh, D. A., Feldmann, R. M., Schroeder, A. M. and Mutel, M. H. (2006). Differential cuticle architecture and its preservation in fossil and extant *Callinectes* and *Scylla* claws. *J. Crustacean Biol.* **26**, 271-282.

Weiner, S. and Addadi, L. (1997). Design strategies in mineralized biological materials. *J. Mater. Chem.* **7**, 689-702.

Weiner, S., Levi-Kalisman, Y., Raz, S. and Addadi, L. (2003). Biologically formed amorphous calcium carbonate. *Connect. Tissue Res.* **44**, 214-218.

Whiteley, N. M. (2011). Physiological and ecological responses of crustaceans to ocean acidification. *Mar. Ecol. Prog. Ser.* **430**, 257-271.

Wickins, J.F. (1984). The effect of hypercapnic sea water on growth and mineralization in penaeid prawns. *Aquaculture* **41**, 37-48.

Figure legends

Fig. 1. Vickers microhardness of the carapace and claw of Tanner crab, *Chionoecetes bairdi* (mean ± s.e.m.). Adult crabs were exposed to one of three pH conditions for two years. Among pH levels, groups marked with different letters are significantly different as shown by Tukey HSD post-hoc analysis. $N = 6–10$; specific values of N can be found in Table S1.

Fig 2. Cuticle thickness of the carapace and claw of Tanner crab, *Chionoecetes bairdi* (mean ± s.e.m.). Adult crabs were exposed to one of three pH conditions for two years. Groups marked with different letters are significantly different as shown by Tukey HSD post-hoc analysis. $N = 7–10$ and specific values of N can be found on Table S2.

Fig. 3. Representative light microscopy images of cuticles of Tanner crab, *Chionoecetes bairdi*, exposed to either ambient pH (8.1) or reduced pH (7.5) for two years. *Left*: carapace interior. Visible erosion (e.g. the darkened region marked by the red arrow, lower left) was apparent on most animals held at pH 7.5, but was not observed in animals held at pH 8.1. *Right*:

pollex exterior. Denticles (white arrow, upper right) were prominent in animals held at ambient pH but were highly worn in animals held at pH 7.5.

Fig. 4. Representative FTIR spectra of powdered cuticle samples from the carapace and claw of Tanner crab, *Chionoecetes bairdi*. Reference spectra for synthetic ACC and biogenic calcite are shown for comparison.

Tables

Table 1. Seawater chemistry parameters (expressed as mean ± s.d.).

	Treatment		
	Ambient	pH 7.8	pH 7.5
pH_F	8.09 ± 0.07	7.80 ± 0.03	7.50 ± 0.03
Temperature (°C)	5.00 ± 1.54	4.94 ± 1.54	4.93 ± 1.53
pCO_2 (µatm)	391.9 ± 65.74	781.17 ± 31.13	1597.15 ± 62.76
DIC (µmol kg^{-1} SW)	2010.76 ± 34.21	2082.18 ± 38.29	2156.84 ± 38.74
HCO_3^- (µmol kg^{-1} SW)	1895.17 ± 41.68	1989.7 ± 37.25	2045.45 ± 36.1
CO_3^{2-} (µmol kg^{-1} SW)	94.72 ± 16.26	50.89 ± 2.99	26.3 ± 1.54
Total alkalinity (µmol kg^{-1} SW)	2135.38 ± 30.3	2119.25 ± 36.29	2112.47 ± 35.98
$\Omega_{Calcite}$	2.31 ± 0.39	1.24 ± 0.07	0.64 ± 0.04

pH and temperature were measured daily (n = 728 per treatment). DIC and alkalinity were measured weekly (n = 101–104 per treatment). Other parameters were calculated (see text).

Table 2. Mixed-model ANOVA table, assessing the effect of hydration and pH on the cuticle microhardness of Tanner crab, *Chionoecetes bairdi*.

	df	F	p
Carapace			
Hydration	**1, 23**	**150.2**	**0.000**
pH	2, 23	2.123	0.143
Hydration X pH	2, 23	2.616	0.095
Claw			
Hydration	1, 21	2.797	0.109
pH	**2, 21**	**7.654**	**0.003**
Hydration X pH	2, 21	1.101	0.351

Significant p-values are shown in bold.

Table 3. Elemental content for the cuticle of Tanner crab, *Chionoecetes bairdi*.

Parameter	**8.1** Mean ± s.e.m.	*N*	**7.8** Mean ± s.e.m.	*N*	**7.5** Mean ± s.e.m.	*N*	ANOVA (F) or Kruskal-Wallis (H)
Carapace							
Ca (% dry mass)	**20.7 ± 0.5 ^{A}**	**10**	**21.2 ± 0.5 ^{A}**	**10**	**18.5 ± 0.4 ^{B}**	**7**	**F_{22}=7.2, p=0.004**
Mg (% dry mass)	**2.40 ± 0.07 ^{A}**	**10**	**2.44 ± 0.06 ^{A}**	**10**	**2.81 ± 0.13 ^{B}**	**7**	**F_{26}=6.6, p=0.005**
Sr (% dry mass)	0.42 ± 0.01	10	0.42 ± 0.01	10	0.49 ± 0.03	7	H_2=4.3, p=0.115
Claw							
Ca (% dry mass)	28.5 ± 0.7	10	28.4 ± 0.4	5	27.0 ± 0.9	7	F_{21}=1.3, p=0.289
Mg (% dry mass)	0.89 ± 0.06	10	1.07 ± 0.08	9	0.94 ± 0.05	7	H_2=5.4, p=0.066
Sr (% dry mass)	0.37 ± 0.01	10	0.37 ± 0.01	9	0.35 ± 0.01	7	F_{25}=2.9, p=0.074

Means ± standard errors (s.e.m.), sample sizes, and ANOVA results are shown. Groups marked with different letters are significantly different as shown by Tukey HSD post-hoc analysis. Significant p-values are shown in bold. Subscripts in the right-most column refer to degrees of freedom.

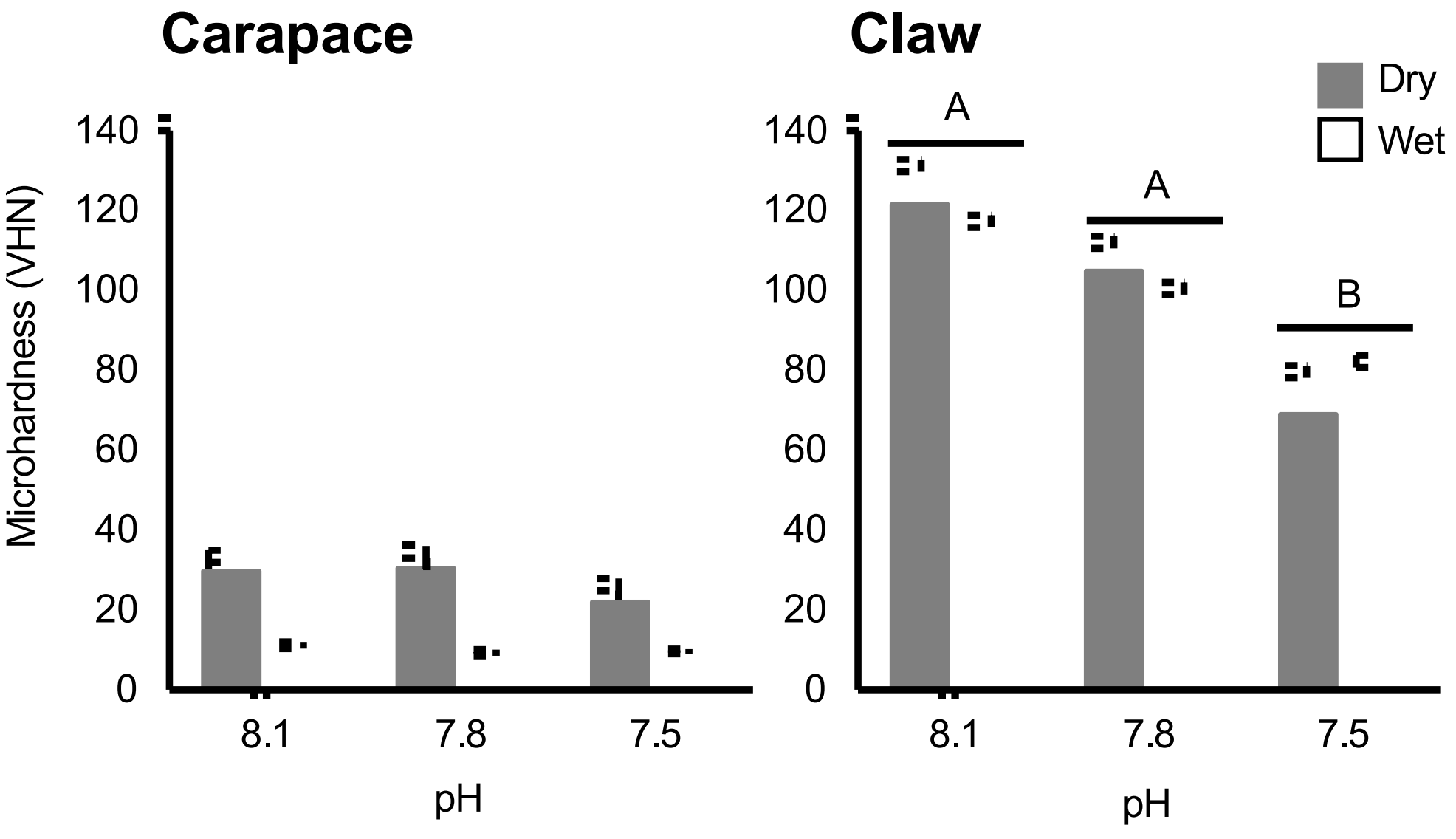
Carapace
Claw
Dry
Wet
Microhardness (VHN)
140
120
100
80
60
40
20
0
A
A
B
8.1
7.8
7.5
pH
8.1
7.8
7.5
pH

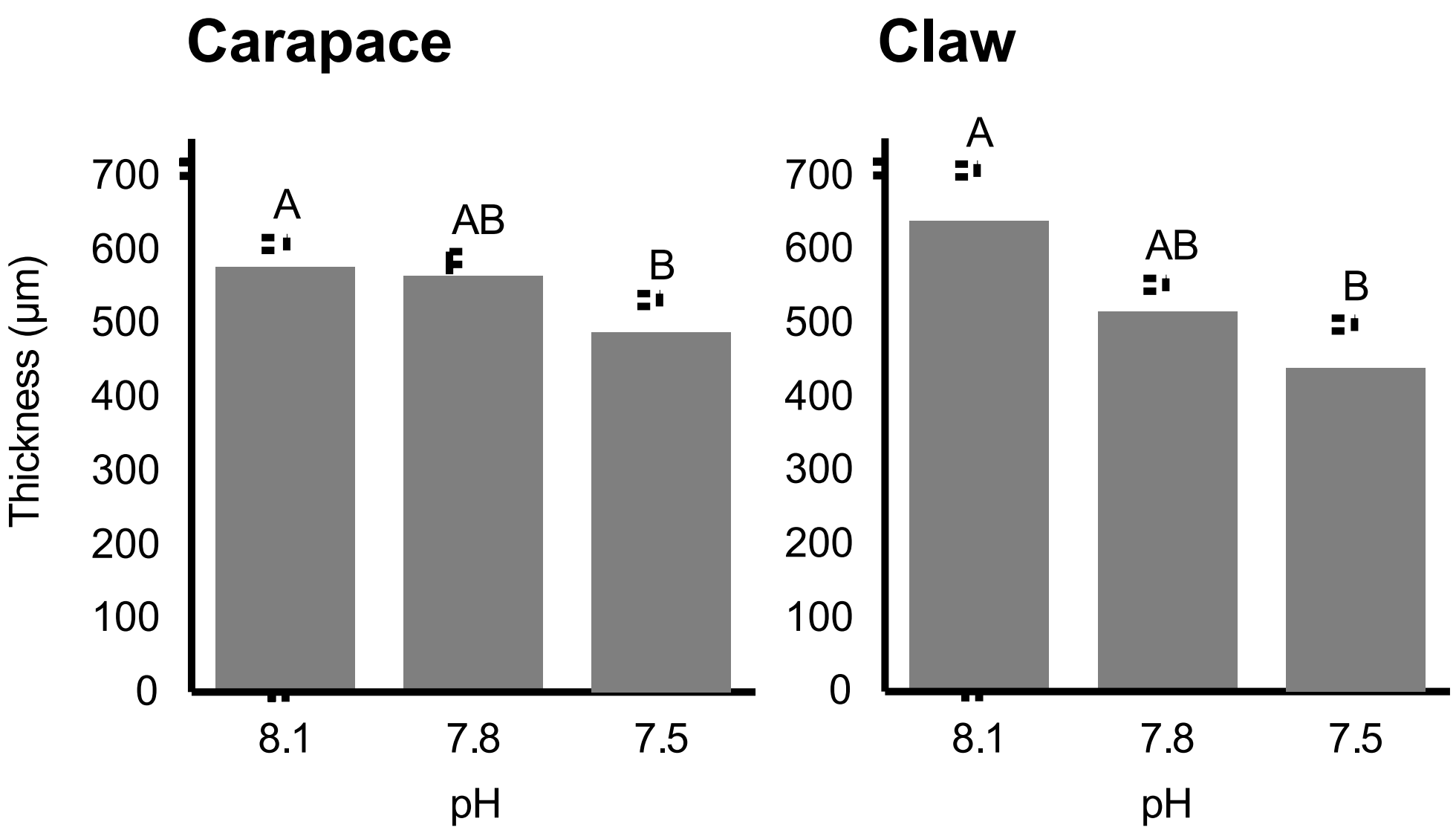
Carapace
Claw
Thickness (µm)
700
600
500
400
300
200
100
0
A
AB
B
8.1
7.8
7.5
pH

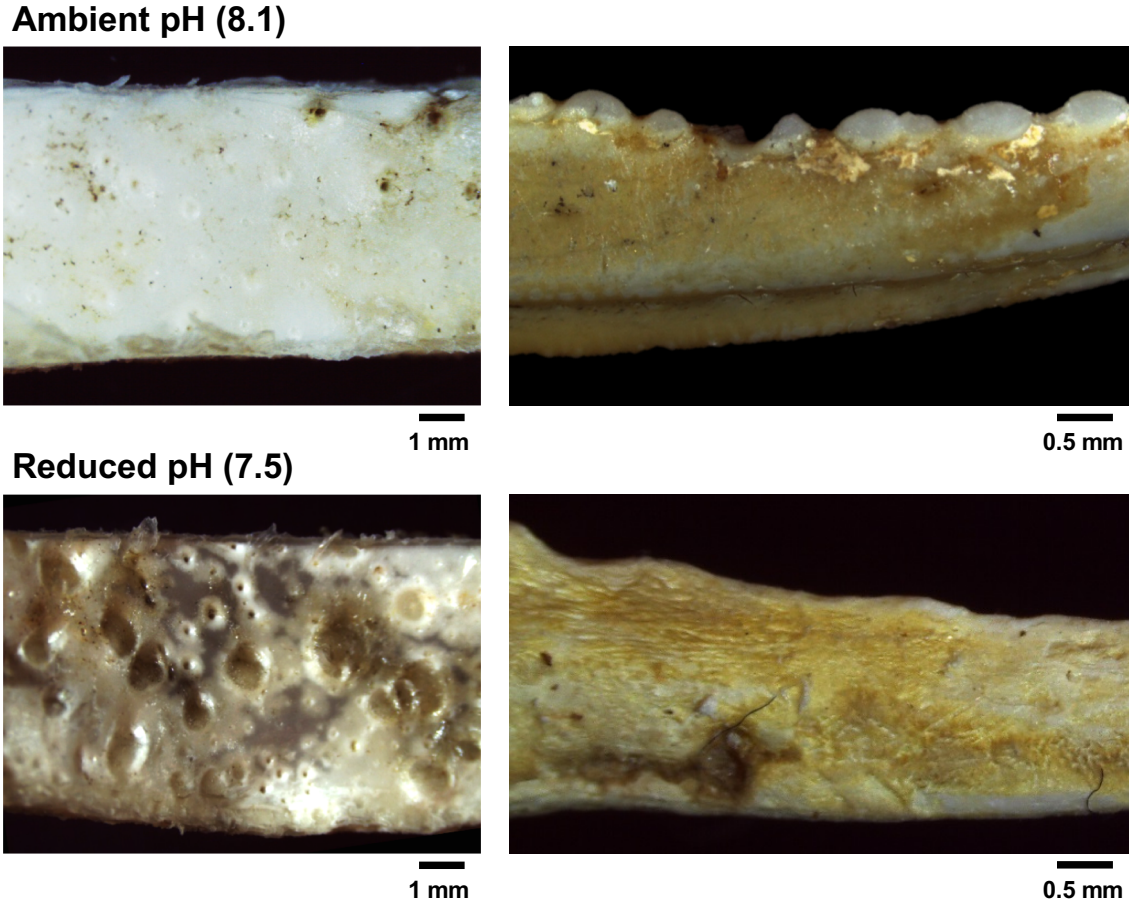
Ambient pH (8.1)
1 mm
0.5 mm
Reduced pH (7.5)
1 mm
0.5 mm

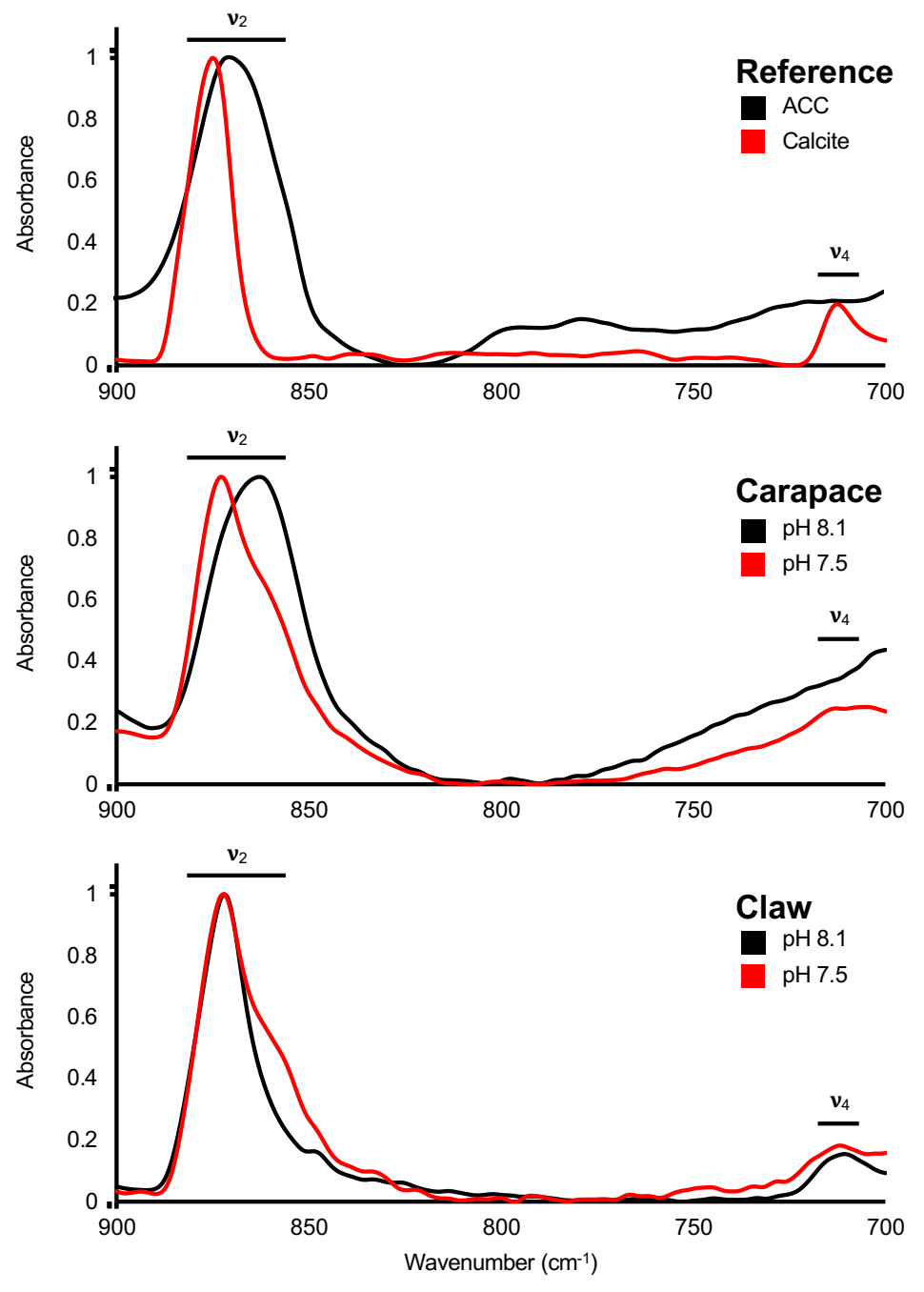
Reference
ACC
Calcite
Carapace
pH 8.1
pH 7.5
Claw
pH 8.1
pH 7.5
ν2
ν4
Absorbance
Wavenumber (cm-1)
1
0.8
0.6
0.4
0.2
0
900
850
800
750
700